doi:10.1246/cl.2010.132

Published on the web January 16, 2010

Monitoring of Photochemical Self-assembly of $[Mo_7O_{24}]^{6-}$ to $\{Mo_{142}\}$-blue Nanoring by Using Mo K-edge XAFS

Yu Mitani,[1] Kazuki Oka,[1] Yoshiyuki Shibata,[1] Kazushi Konishi,[1] Diaa M. Obaid,[2] Eri Ishikawa,[2] Yasuo Izumi,*[1] and Toshihiro Yamase*[2,3]

[1]*Department of Chemistry, Graduate School of Science, Chiba University, 1-33 Yayoi, Inage-ku, Chiba 263-8522*
[2]*Chemical Resources Laboratory, Tokyo Institute of Technology, 4259 Nagatsuta, Midori-ku, Yokohama 226-8503*
[3]*(Inc.) MO device, 2-14-10 Kanaiwa-higashi, Kanazawa 920-0335*

(Received November 25, 2009; CL-091045; E-mail: yizumi@faculty.chiba-u.jp)

The UV-induced self-assembly of $[Mo_7O_{24}]^{6-}$ to 28-electron-reduced $\{Mo_{142}\}$ at pH 3.4 was monitored by Mo K-edge XAFS spectra of photolytes. The EXAFS curve fit analysis indicates that the accumulation of $[MoO_4]^{2-}$ in an equilibrium with $\{Mo_8\}$ was accompanied by the formation of two-electron-reduced $\{Mo_{14}\}$, and the subsequent construction of the $\{Mo_{20}\}$ and $\{Mo_{21}\}$ building blocks provided $\{Mo_{142}\}$ through their reductive condensation.

Twenty-eight-electron-reduced Mo-blue nanorings, $[Mo_{142}O_{418}(OH)_{14}(H_2O)_{58}]^{26-}$ and $[Mo_{154}O_{448}(OH)_{14}(H_2O)_{70}]^{14-}$,[1–3] have attracted attention in host–guest chemistry,[1,3] shape-selective catalysis,[4] and molecular magnetism.[5] The former shows a defect ring due to a removal of six *linkers* from an intact ring of the latter comprising fourteen $[Mo_2O_5(H_2O)_2]^{2+}$ *linkers*.[1] The same type of carboxylate-coordinated Mo-blue ring, $[Mo_{142}O_{419}(OH)_{10}(H_2O)_{49}(CH_3CO_2)_5(C_2H_5CO_2)]^{30-}$ ($\equiv\{Mo_{142}\}$), prepared photochemically in the presence of acetic acid at pH 3.4, has provided a good model for clarification of the mechanism of the self-assembly to the Mo-blue nanorings,[4] which is essential for the molecular design of Mo-blue-based supramolecules.

$[Mo_7O_{24}]^{6-}$ ($\equiv\{Mo_7\}$) and β-$[Mo_8O_{26}]^{4-}$ ($\equiv\{Mo_8\}$) as dominant species in aqueous solutions of molybdates at pH 3–6 have been identified by ^{17}O and ^{95}Mo NMR spectra which distinguish between terminal and bridging O atoms and among three types of Mo sites, respectively.[6,7] Two-electron-reduced Mo-blue, $[Mo_{14}O_{46}]^{10-}$ ($\equiv\{Mo_{14}\}$) as a condensed dimer of $\{Mo_7\}$, is produced through one-electron reduction of $\{Mo_7\}$ in the photolysis of $\{Mo_7\}$ at pH 5.4.[8] Recently, an involvement of multielectron-reduced $\{Mo_{37}\}$–$\{Mo_{42}\}$ intermediates through $\{Mo_{20}\}$ and $\{Mo_{21}\}$ building blocks in the photochemical self-assembly of $\{Mo_7\}$ to $\{Mo_{142}\}$ at pH 3.4 has been shown by ESI-MS analysis.[9] To obtain mechanistic details of this self-assembly, the electronic structure of the local Mo sites has been monitored by Mo K-edge XAFS. In this letter, it is strongly supported that the $\{Mo_{20}\}$ and $\{Mo_{21}\}$ building blocks are produced through the reaction of $\{Mo_{14}\}$ with $[MoO_4]^{2-}$ ($\equiv\{Mo_1\}$) in an equilibrium with $\{Mo_8\}$.

$[NH_4]_6[Mo_7O_{24}]\cdot 4H_2O$ (**1**) (0.40 g, 0.31 mmol) was dissolved in water (20 mL), and acetic acid as electron donor was added until the pH level of the solution became 3.4. The resultant solution was exposed to UV light from a 500-W xenon lamp. Each photolyte sample from 6-, 12-, 24-, 48-, and 72-h photolyses was kept in the dark and transported to the beamline.

Mo K-edge XAFS spectra were measured at 30–290 K in transmission mode on beamline NW10A of PF-AR, KEK. At beamline, the solutions were transferred without contact to air to an XAFS cell equipped with 25-μm-thick Kapton windows on both sides. XAFS analyses were done by use of XDAP 2.2.7 (XAFS Services International). Multiple shell curve fit analyses used the Fourier-filtered k^3-weighted EXAFS data (k: wavenumber of photoelectrons).[10] The fit parameters for Mo=O and Mo–O bonds were extracted from the EXAFS data measured for $K_2[MoO_4]$ (**2**).[11] The fit parameters for Mo···Mo atomic distances were theoretically generated using FEFF 8.4[12] based on the crystal structure of **1**.[13] Typical interatomic distances for Mo=O, Mo–O, and Mo···Mo are 1.66–1.76, 1.85–2.55, and 3.20–4.04 Å for polyoxomolybdates. The best-fit results of Mo K-edge EXAFS[14] for photolytes are summarized in Table 1. Coordination numbers (N) of Mo=O, Mo–O, and Mo···Mo pairs for the 0-h photolyte (before the photolysis) were 2.1, 4.1, and 3.7, respectively, suggesting partial formation of $\{Mo_1\}$ in an equilibrium with $\{Mo_8\}$ and $\{Mo_7\}$.[15] If the population ratio between $\{Mo_8\}$ (or $\{Mo_7\}$) and $\{Mo_1\}$ was 85:15, the calculated N values were 2.0, 3.7, and 3.6, respectively. Interestingly, the 6-h photolysis showed an increase of the N(Mo=O) value (2.6) and a decrease of the N(Mo–O) and N(Mo···Mo) values (3.1 and 2.7). If the population ratio of $\{Mo_{14}\}$ (or $\{Mo_7\}$) and $\{Mo_1\}$

Table 1. Best-fit results to Mo K-edge EXAFS spectra of photolytes at various duration (h) of photolysis and site structural parameters of compounds[a]

Photolytes and Compds	Mo=O[b]		Mo–O[c]		Mo···Mo		Goodness of fit
	N	R(Å)	N	R(Å)	N	R(Å)	
0	2.1 (±0.7)	1.669 (±0.015)	4.1 (±0.3)	1.932 (±0.018)	3.7 (±0.2)	3.314 (±0.004)	2.0×10^4
6	2.6 (±0.9)	1.648 (±0.008)	3.1 (±0.5)	1.918 (±0.018)	2.7 (±0.5)	3.308 (±0.006)	3.1×10^4
12	2.2 (±0.6)	1.665 (±0.015)	4.1 (±0.2)	1.925 (±0.012)	4.1 (±0.2)	3.329 (±0.013)	3.2×10^4
24	1.8 (±0.2)	1.659 (±0.008)	4.3 (±0.1)	1.948 (±0.013)	4.5 (±0.4)	3.340 (±0.004)	3.5×10^4
48	1.7 (±0.4)	1.657 (±0.012)	4.9 (±0.1)	1.941 (±0.010)	4.6 (±0.6)	3.362 (±0.004)	3.7×10^4
72	1.5 (±0.5)	1.657 (±0.015)	4.6 (±0.7)	1.938 (±0.013)	4.9 (±0.4)	3.360 (±0.002)	5.8×10^4
$\{Mo_1\}$(**2**)[d]	4	1.76					Ref. 11
$\{Mo_7\}$(**1**)[d]	1.7	1.73	4.3	2.06	3.4	3.31	Ref. 13
$\{Mo_8\}$[d]	1.7	1.70	4.3	2.11	4.2	3.35	Ref. 4
$\{Mo_{14}\}$[d]	1.4	1.71	4.6	2.08	3.7	—[f]	Ref. 8
$\{Mo_{20}\}$[e]	1.8	—[f]	4.2	—[f]	4.3	—[f]	Ref. 4
$\{Mo_{142}\}$[d]	1.5	1.70	4.6	1.97	4.9	—[f]	Ref. 4

[a]Fit errors were indicated in parentheses. [b]For terminal Mo=O (double or single and a half) bonds. [c]For Mo–OH, Mo–OH_2, and bridging Mo–O–Mo bonds. [d]Based on X-ray crystallographic data for authentic samples. [e]Based on hypothetical fragment structure from $\{Mo_{142}\}$. [f]Exact values were difficult to obtain due to bond strain.

was 7:3, N(Mo=O), N(Mo–O), and N(Mo···Mo) were 2.2, 3.2, and 2.6, respectively, which are close to the values fitted for the 6-h photolyte comprising high amounts of $\{Mo_{14}\}$ derived from $\{Mo_7\}$.[1] A similarity in EXAFS values between $\{Mo_{14}\}$ and $\{Mo_7\}$ with similar coordination of Mo sites implies that EXAFS is unexpectedly insensitive to the $Mo^{VI} \rightarrow Mo^{V}$ photoreduction.[16]

For more than 12-h photolytes, the N(Mo=O) value decreased to 1.5 at 72-h photolysis, while N(Mo–O) and N(Mo···Mo) values increased to 4.6 and 4.9, respectively (Table 1). The bond lengths (R) for Mo=O and Mo–O remained nearly constant within 0.021 and 0.030 Å, respectively, throughout the photolysis. On the other hand, the Mo···Mo distances elongated gradually from 3.308 Å at 6 h to 3.362 Å at 48 h ($\Delta = 0.054$ Å), due to an increase of the bond strain with increasing ring geometry to $\{Mo_{142}\}$.[1]

Assuming that the 12-h photolyte consisted 90% of $\{Mo_{20}\}$ or $\{Mo_{21}\}$ (higher nuclearity species than $\{Mo_{14}\}$) and 10% $\{Mo_1\}$, the values estimated for N(Mo=O), N(Mo–O), and N(Mo···Mo) were 2.0, 3.8, and 3.9, respectively, which were in good agreement with the result fitted for the 12-h photolyte (Table 1) but only based on estimated N values, the possibility of inclusion of $\{Mo_8\}$ cannot be excluded. Together with the fact that N values for the three interatomic lengths at the 24-h photolysis are close to the values for $\{Mo_{20}\}$ (Table 1), the EXAFS best-fit results support the formation of $\{Mo_{20}\}$ and $\{Mo_{21}\}$ building blocks during 12–24 h photolysis. Also, N values for the three lengths for the 72-h photolyte are consistent with those for $\{Mo_{142}\}$, suggesting the formation of $\{Mo_{142}\}$ through the reductive cyclic heptamerization of the $\{Mo_{20}\}$ and $\{Mo_{21}\}$ building blocks during 24–72 h photolysis. Although the precipitation of $\{Mo_8\}$ as $[Me_3NH]^+$ salt from the 72-h photolyte strongly indicates the equilibrium between $\{Mo_8\}$ and $\{Mo_1\}$ at pH 3.4,[4,15] it should be noted that the dominant molybdates in the 72-h photolyte are likely to be $\{Mo_{142}\}$ and $\{Mo_8\}$. The values of R(Mo=O) and R(Mo–O) for photolytes were always smaller than for crystals (Table 1), implying more covalent bonding in solution than in crystal. The reason is not clear at present. Peaks associated with further distant Mo sites than Mo···Mo were not clearly observed.

A shoulder peak at 19994.5 eV due to the dipole-forbidden electronic Mo 1s → 4d transition near the Mo K absorption edge reflects inversion symmetry of Mo center,[17] and its intensities for **2** and MoO_3 corresponding to MoO_4-tetrahedral and MoO_6-octahedral compounds were 0.43 and 0.31, respectively. The peak intensity of the photolyte was almost unchanged during 6-h photolysis (0.31) and decreased during 6–72 h photolysis (0.27), supporting an increase of the MoO_4-tetrahedra during 6-h photolysis and their decrease during further photolysis with a compensating increase of the MoO_6-octahedra through $\{Mo_{142}\}$ formation. The 1s → 4d peak for $\{Mo_{142}\}$ crystal is also shown in Figure 1.

Stepwise photoreaction pathway of $\{Mo_7\}$ to $\{Mo_{142}\}$ at pH 3.4 is consistent to the theory of the condensation as depicted in Scheme 1: $\{Mo_7\}$ is in equilibrium with $\{Mo_8\}$ through the dissociation to $\{Mo_1\}$.[15] The accumulation of $\{Mo_1\}$ through the dissociation of $\{Mo_8\}$ resulting from the photochemical formation of $\{Mo_{14}\}$ was indicated by EXAFS data for the 6-h photolyte (ca. 30% of $\{Mo_1\}$). Subsequent decrease of the $\{Mo_1\}$ population for the 12-h photolyte

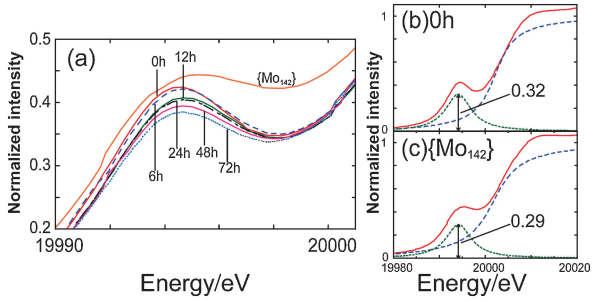

Figure 1. Normalized Mo K-edge XANES spectra. Change of the Mo 1s → 4d pre-edge region during the photolysis (a). Fit evaluation of 1s → 4d peak intensity (0.32 and 0.29) for 0-h photolyte (b) and $\{Mo_{142}\}$ crystal (c).

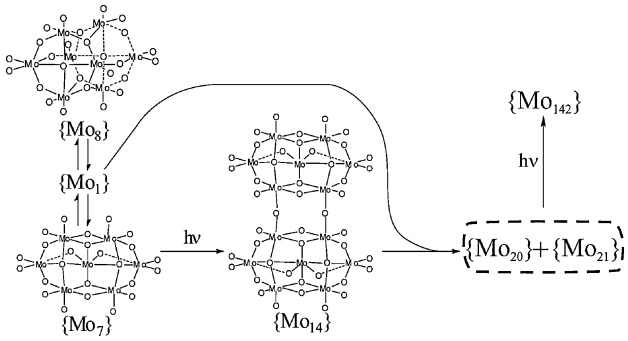

Scheme 1. Pathway to $\{Mo_{142}\}$ through $\{Mo_{20}\}$ and $\{Mo_{21}\}$.

supports the formation of the $\{Mo_{20}\}$ and $\{Mo_{21}\}$ building blocks through the reaction of $\{Mo_1\}$ with $\{Mo_{14}\}$, followed by the heptameric cyclic condensation of the building blocks to $\{Mo_{142}\}$ during 24- to 72-h photolysis.[4,8]

References and Notes

1 T. Yamase, P. V. Prokop, *Angew. Chem., Int. Ed.* **2002**, *41*, 466.
2 A. Müller, E. Krickemeyer, H. Bögge, M. Schmidtmann, C. Beugholt, S. K. Das, F. Peters, *Chem.—Eur. J.* **1999**, *5*, 1496.
3 A. Müller, S. Q. N. Shah, H. Bögge, M. Schmidtmann, *Nature* **1999**, *397*, 48.
4 T. Yamase, Y. Yano, E. Ishikawa, *Langmuir* **2005**, *21*, 7823.
5 H. Imai, T. Akutagawa, F. Kudo, M. Ito, K. Toyoda, S. Noro, L. Cronin, T. Nakamura, *J. Am. Chem. Soc.* **2009**, *131*, 13578.
6 M. A. Fedotov, R. I. Maksimovskaya, *J. Struct. Chem.* **2006**, *47*, 952.
7 R. I. Maksimovskaya, G. M. Maksimov, *Inorg. Chem.* **2007**, *46*, 3688.
8 T. Yamase, *J. Chem. Soc., Dalton Trans.* **1991**, 3055.
9 T. Ito, T. Yamase, *Eur. J. Inorg. Chem.* **2009**, 5205.
10 Y. Izumi, K. Konishi, M. Tsukahara, D. M. Obaid, K. Aika, *J. Phys. Chem. C* **2007**, *111*, 10073.
11 B. M. Gatehouse, P. Leverett, *J. Chem. Soc. A* **1969**, 849.
12 A. L. Ankudinov, B. Ravel, J. J. Rehr, S. D. Conradson, *Phys. Rev. B* **1998**, *58*, 7565.
13 H. T. Evans, Jr., B. M. Gatehouse, P. Leverett, *J. Chem. Soc., Dalton Trans.* **1975**, 505.
14 EXAFS χ-function, associated Fourier transform, and fits are in Supporting Information. Supporting Information is available electronically on the CSJ-Journal Web site, http://www.csj.jp/journals/chem-lett/index.html.
15 F. A. Cotton, G. Wilkinson, C. A. Murillo, M. Bochman, *Advanced Inorganic Chemistry*, 6th ed., Wiley-Interscience, **1999**, pp. 920–951.
16 S. P. Cramer, P. K. Eidem, M. T. Paffett, J. R. Winkler, Z. Dori, H. B. Gray, *J. Am. Chem. Soc.* **1983**, *105*, 799.
17 Y. Izumi, *Stud. Surf. Sci. Catal.* **2000**, *130*, 3201.

